

**SYNTHESIS OF MESOPOROUS ALUMINA FROM RED MUD****Eka Putra Ramdhani\*<sup>1</sup>, Suprpto<sup>1</sup>, Didik Prasetyoko<sup>1</sup>, Hartati<sup>2</sup>**<sup>1</sup>*Department of Chemistry, Faculty of Science, Institut Teknologi Sepuluh Nopember (ITS),*<sup>2</sup>*Department of Chemistry, Faculty of Science and Technology, Airlangga University*\*[eka.putra12@mhs.chem.its.ac.id](mailto:eka.putra12@mhs.chem.its.ac.id), [denni\\_yata@yahoo.com](mailto:denni_yata@yahoo.com)**Abstract**

Mesoporous Al<sub>2</sub>O<sub>3</sub> has been successfully synthesized by using calcined red mud as raw material and cetyltrimethylammonium bromide (CTAB) as template at room temperature. The effect of CTAB ratio on the structural and textural properties of mesoporous Al<sub>2</sub>O<sub>3</sub> was investigated. In this study, Al<sub>2</sub>O<sub>3</sub> from red mud was separated by centrifugation, dissolving and precipitation methods. Firstly, HCl 6N solution was added to separate SiO<sub>2</sub>. Subsequently, other impurities was separated by addition of NaOH 5N solution. Physical properties of obtained samples were characterized by X-ray diffraction (XRD), N<sub>2</sub> adsorption-desorption, transmission electron microscopy (TEM), scanning electron microscopy (SEM) with energy-dispersive X-ray analysis (EDAX). The results indicated that red mud has a great potential as mesoporous alumina. XRF result of red mud from Bintan Kepulauan Riau shown that it most contains of Al<sub>2</sub>O<sub>3</sub> 29 wt%, Fe<sub>2</sub>O<sub>3</sub> 44.86 wt%, and SiO<sub>2</sub> 20.3 wt%. XRD results confirmed that mesoporous Al<sub>2</sub>O<sub>3</sub> was obtained after calcined samples at 550 °C. BET results indicated that all samples had mesoporous structures with BET surface area of 241 m<sup>2</sup>/g and pore size of 3.820 nm. In addition, the reaction mechanism involved in the process was proposed and discussed.

**Key words:** Mesoporous alumina, red mud, CTAB**INTRODUCTION**

Red mud is a residue or waste material derived from the processing of bauxite to alumina production. Globally, there are about 70 million tons of red mud are worldwide produced annually. Averagely, 0.3–2.5 tons of red mud maybe generated after producing 1 ton of alumina depending on the grade of ore used [1]. For solid waste, red mud will be found in the form of wet or dry mud which is collected in a pond. The magnitude of waste generated by industry clearly demonstrates the need for future developments that find a beneficial use for this material.

Red mud is comprised of iron oxides, titanium oxides, silicon oxides and undissolved alumina, along with a wide range of other oxides depending on the country of origin [2]. Trace levels of metal oxides, such as arsenic, cadmium, chromium, copper, gallium, lead, mercury, nickel and in some cases thorium and uranium, are of particular concern [3]. Apart from heavy metal contamination, the alkalinity of red mud also constrains viable applications due to the cost of neutralization. Alkalinity in the residue exists in both solid and solution as: (1) entrained liquor (sodium hydroxide, sodium aluminate and sodium carbonate), (2) calcium compounds, such as hydrocalumite, tri-calcium aluminate and lime, and (3) sodalite ((NaAlSiO<sub>4</sub>)<sub>6</sub>(Na<sub>2</sub>X)), where X can be SO<sub>4</sub><sup>2-</sup>, CO<sub>3</sub><sup>2-</sup>, Al(OH)<sup>4-</sup> or Cl<sup>-</sup> [4].

The recovery of a significant quantity of valuable components from the red mud is difficult, as they are locked up in complex mineral phases which are very fine grained and quite

alkaline. Recovery of alumina from red mud can be done through several methods such as the addition of  $\text{MgO} + \text{Na}_2\text{CO}_3$  through sintering process [5], mild hydro-chemical processes [6], the addition of acid ( $\text{HCl}$ ,  $\text{H}_2\text{SO}_4$ , and  $\text{HNO}_3$ ) [7], hydrothermal processes [8], and the process of reduction sintering [9].

Mesoporous  $\text{Al}_2\text{O}_3$  has excellent properties such as highly uniform channels, large surface area and narrow pore size distribution. It has been widely used as adsorbents, catalysts supports, ceramics, heat insulating materials, and reinforcements for composite materials [10]. Because of such excellent properties, many attempts have been made to prepare mesoporous alumina by using different methods, such as evaporation- induced self-assembly (EISA) [11], hard or soft template self- assembly [12] etc. Some expensive aluminum alkoxide or inorganic salts as aluminum sources were used in the mentioned methods. However, among these synthesis routes, the processes were either complicated or uneconomical, which limits large-scale application in industry.

In our experiment system, we move the impurity elements completely by making  $\text{AlCl}_3$  solution convert to  $\text{NaAlO}_2$  solution. Furthermore, to the best of our knowledge, mesoporous  $\text{Al}_2\text{O}_3$  was succeed synthesized from kaolin using CTAB as template [13], but no reports are available about synthesis of mesoporous alumina from red mud using CTAB as template at room temperature to date. Here in we present an accessible route for the synthesis of mesoporous alumina from Red Mud We used leachate of Red Mud as Al resource, CTAB as template, synthesized mesoporous alumina at room temperature.

## RESEARCH METHOD

### 1. Materials

The raw material powders of Red Mud were obtained from Bintan Island of Indonesia, its chemical composition was (mass%):  $\text{SiO}_2$ , 20.3;  $\text{Al}_2\text{O}_3$ , 29;  $\text{Fe}_2\text{O}_3$ , 44.86;  $\text{TiO}_2$ , 3.04;  $\text{CaO}$ , 0.28;  $\text{K}_2\text{O}$ , 0.37;  $\text{P}_2\text{O}_5$ , 0.51;  $\text{V}_2\text{O}_5$ , 0.07;  $\text{Cr}_2\text{O}_3$ , 0.101;  $\text{NiO}$  0.62;  $\text{CuO}$ , 0.12;  $\text{ZnO}$ , 0.04;  $\text{ZrO}_2$ , 1.3;  $\text{As}_2\text{O}_3$ , 0.15;  $\text{Re}_2\text{O}_7$ , 0.2. and ignition loss, 20.59. Cetyltrimethylammoniumbromide (CTAB), sodium hydroxide (analytical grade), Chloride Acid (analytical grade), aquadest.

### 2. Procedure

100 gr Red Mud was watered and stirred at low speed to remove some  $\text{Fe}_2\text{O}_3$  contain by of gravitational principle. 50 gr solids from top layer was collected and treated in 6N  $\text{HCl}$  solution (solid/liquid ratio 1:5, g/ml) at 90 °C for 2 h with stirring. The obtained suspension was filtered and the filtrate was collected as Al source for synthesis of mesoporous alumina.  $\text{NaOH}$  solution (5N) was dropped into filtrate from previous procedure with vigorous stirring until  $\text{AlCl}_3$  transformed into  $\text{NaAlO}_2$  completely. Some impurity elements ( $\text{Fe}^{3+}$ ,  $\text{Mg}^{2+}$ , etc.) formed precipitates that could be removed by filtering, and then  $\text{NaAlO}_2$  solution was obtained. Subsequently,  $\text{HCl}$  solution (6N) was added to the  $\text{NaAlO}_2$  solution with magnetic stirring until the pH was 7. The precipitate was collected and washed with deionized water. 1 g CTAB was pre-dissolved in 50 ml of deionized water at 60 °C. The moist solid obtained was mixed with CTAB solution with vigorous stirring for 1h. After that, the suspension was aged for 72 h at room temperature. The final white products were recovered by filtration, washed with deionized water, and dried at 120 °C. Then the as-synthesized samples were calcined at 550 °C for 6 h.

### 3. Characterization

Powder X-ray diffraction pattern were collected on Phillips Expert with  $\text{CuK}\alpha$  radiation ( $\lambda = 1,54056 \text{ \AA}$ ), voltage 40 kV, 30 mA and  $2\theta = 5\text{-}50^\circ$ . The surface area (calculated by BET method), pore size distribution (calculated by BJH method) and pore volume were obtained at -196 °C using an Quantachrome Instrument. Solids were characterization by Scanning electron microscope (SEM) images operated at an acceleration voltage of 20.00 kV and work distance of

9 mm. Compositional analysis were performed using energy-dispersive X-ray analyzer attached to the microscope (SEM-EDX) for Al, Fe, Si, O, Br. Transmission electron microscopy (TEM) images were obtained on a JEOL JEM 1400 (UGM Yogyakarta - Indonesia).

## RESULT AND DISCUSSION

### 1. XRD Analysis

The XRD diagram of red mud is shown as Fig. 1(a). It can be known that the main mineral phases of red mud are Dicalcium Silicate ( $\text{Ca}_2\text{SiO}_4$ ), Calcite ( $\text{CaCO}_3$ ), Perovskite Oxide ( $\text{CaTiO}_3$ ), Magnetite ( $\text{Fe}_3\text{O}_4$ ) and Hematite ( $\text{Fe}_2\text{O}_3$ ), etc. Fig. 1(b) shows XRD patterns of  $\text{Al}_2\text{O}_3$  precursor and calcined samples obtained at  $550^\circ\text{C}$ . No diffraction peaks were detected in XRD patterns in samples with various CTAB concentrations. It indicated that mesoporous was obtained in samples with various CTAB concentrations. The absence of diffraction lines characteristic to an ordered oxide phase was in accord with a mesostructure with amorphous framework walls.

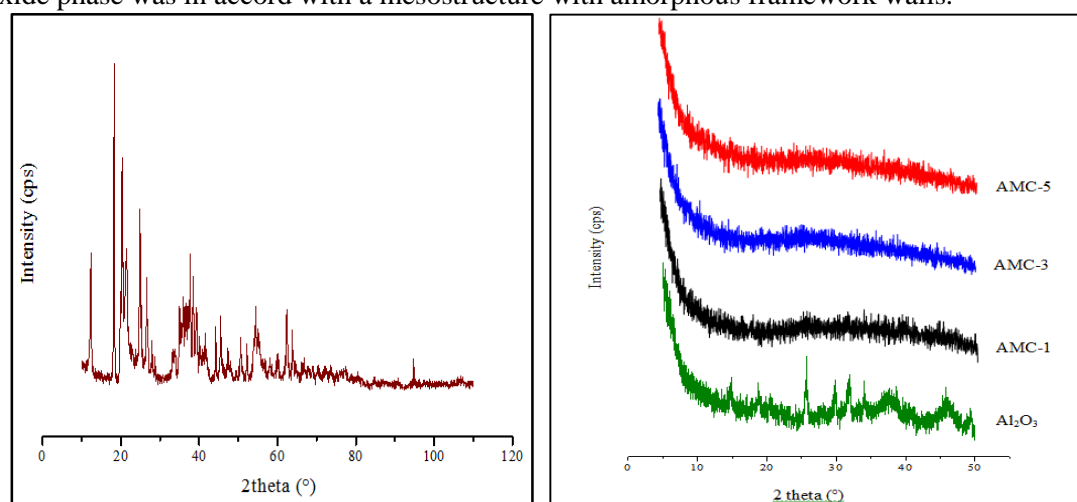


Figure 1. XRD pattern of (a) red mud and (b) as-synthesized and calcined samples

### 2. BET and Pore Sizes Analysis

Adsorption parameters such as the BET specific surface area, total pore volume and pore size, calculated from nitrogen adsorption data, were summarized in Table 1. The surface areas for all samples were decreased with the increase of CTAB/Al from 0.32 to 1.60. When the CTAB/Al ratio was increased to 1.6, surface area were decreased from 241 to 216  $\text{m}^2/\text{g}$ . However when the CTAB/Al ratio was increased to 1.6, pore volume of synthesized materials were decreased to 0.048  $\text{cm}^3/\text{g}$  and mesopore volume decreased from 61.452 to 6.114  $\text{m}^2/\text{g}$ . On the basis of the experimental fact that no significant change in the average pore size was observed in the CTAB/Al ratio range from 0.32 to 1.60. Under assumption that the size of CTAB micelles is fixed, the d-spacing should be reduced with increasing the CTAB/Al ratio because of the increase in the number density of micelles [14].

There were mesopore distribution for all samples could be observed in Fig. 2. The  $\text{N}_2$  adsorption-desorption isotherms for all samples are typical type IV isotherms, no significant difference in hysteresis loop observed, which supported that the prepared alumina has similar and monodisperse pore structure. At the relative pressure ( $P/P_0$ ) range from 0.4 to 0.6, the nitrogen-adsorption was saturated and this saturation pressure was not influenced by the CTAB/Al ratio, which means that the prepared alumina particles have mesopores and no significant change in the average pore size occur as the CTAB/Al ratio changes. Moreover, due to the present of CTAB in

the reaction media during the gel formation, CTAB micelles have incorporated within the gel and thereby facilitate the process of template formation.

Table 1. Porous properties of mesoporous alumina

Samples	CTAB/Al Ratio	$d_{\text{BJH}}$ (nm)	$S_{\text{BET}}$ ( $\text{m}^2/\text{g}$ )	$S_{\text{meso}}$ ( $\text{m}^2/\text{g}$ )	$V_{\text{p}}$ ( $\text{cm}^3/\text{g}$ )
AMC-1	0.32	3.820	241	61.452	0.107
AMC-3	0.96	3.822	223	37.645	0.056
AMC-5	1.60	3.817	216	6.114	0.048

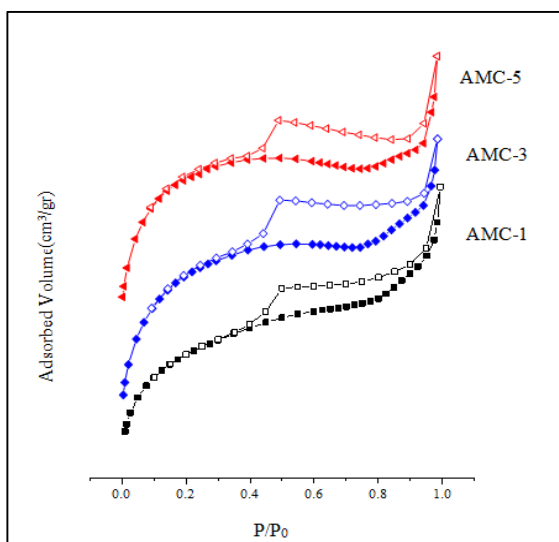


Figure 2.  $\text{N}_2$  Adsorption-Desorption Isotherms of Samples

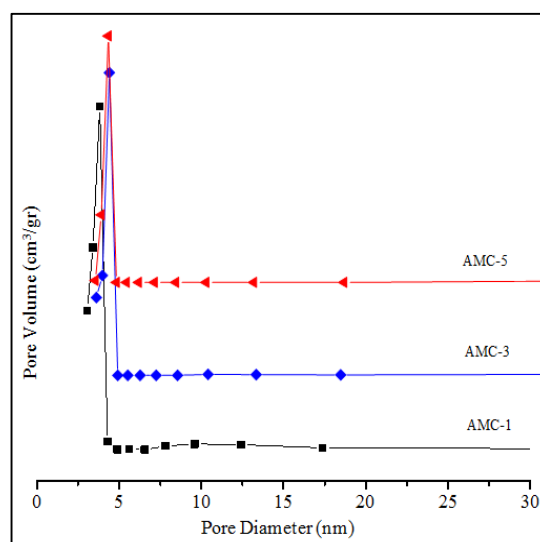


Figure 3. Pore Size Distribution of Samples Obtained by BJH Method

### 3. TEM Analysis

Fig. 4 presented TEM micrographs of obtained mesoporous alumina sample of AMC-3 with CTAB/Al ratio of 0.96 and it was aggregated by nanometer particles. Therefore, the pores of AMC-3 were typical worm-hole framework structures without apparent order in the pore arrangement [15], in good agreement with the absence of peak in the XRD patterns (Fig.1b).

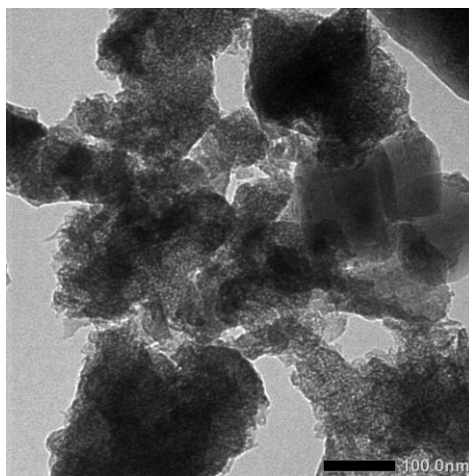


Figure 4. TEM image of AMC-3

#### 4. SEM-EDX Analysis

SEM images and energy-dispersive X-ray analysis for mesoporous alumina samples were shown in Fig. 4. According to the images, the morphologies of the mesoporous alumina changed slightly along with increasing CTAB/Al ratio.

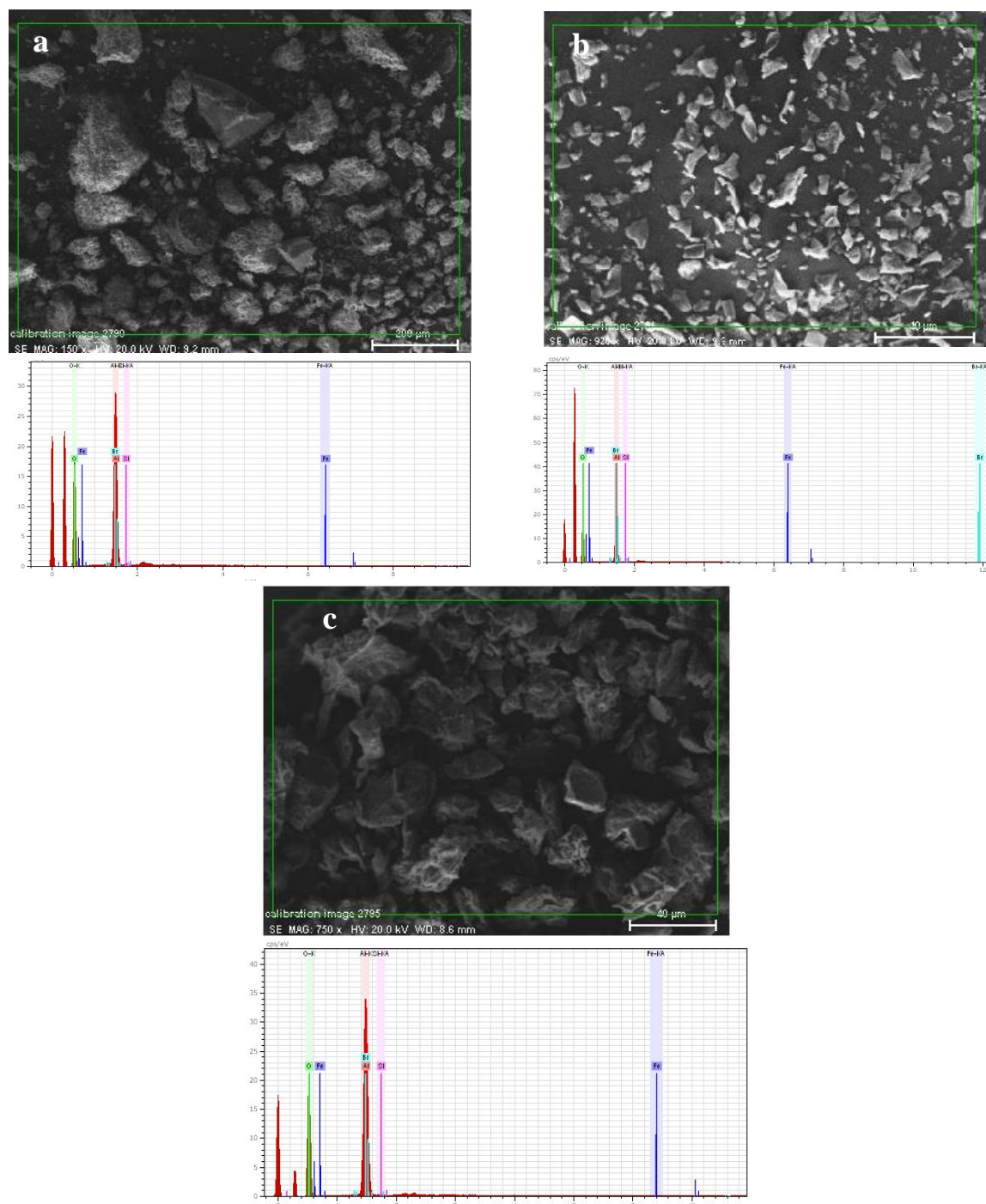


Figure 4. SEM images of mesoporous alumina samples : a) AMC-1, b) AMC-3 and c) AMC-5

Results obtained by XRD were confirmed with those of SEM. This technique was used to determine the morphology and the particle size. Fig. 3 compares the SEM-EDX images of the AMC-1, AMC-3, and AMC-5 samples. Images of all sample consist of amorphous aggregates of alumina. However, increasing the CTAB/Al ratio from 0.32 to 1.96 not resulted a crystalline alumina, and there were wide range particle size in samples. Its boundary between the particles could be clearly observed by SEM. EDX spectrum results show that the samples composed of elements - elements that are used as precursors, namely Fe, Si, Al, O, and Br. This indicates that there are no other elements that are formed during the synthesis process. In addition, low composition of Fe and Si in as-synthesized material confirmed that those material were succeed removed by extraction methods. There were few Br in samples indicated that not all CTAB were removed during calcination at 550 °C.

## CONCLUSION

In conclusion, mesoporous alumina has been successfully synthesized by using leachate of red mud as Al resource and CTAB as surfactant. The as-synthesized samples became mesoporous Al<sub>2</sub>O<sub>3</sub> after removing the template. The concentration of CTAB was closely related to the formation of the micelle and system entropy, which influenced the formation of mesopore and porous properties significantly, especially the BET areas and pore volumes. Among the obtained samples, AMC-1 showed the best mesoporous features with surface areas of 241 m<sup>2</sup>/g and pore volumes of 0.107 cm<sup>3</sup>/g. Therefore, Al<sub>2</sub>O<sub>3</sub> with highly well-organized meso-structure and narrow pore-size distribution is a potential material in adsorptive and catalytic applications.

## ACKNOWLEDGEMENTS

The authors would like to acknowledge the Ministry of Research and Higher Education, Indonesia, under “PUPT” research grant No. 003246.18/IT2.11/PN.08/2015.

## REFERENCES

- [1] Jankovic, B., Smiciklas, I., Stajic-Trosic, J., Antonovic, D., (2013). Thermal characterization and kinetic analysis of non-isothermal decomposition process of Bauxite Red Mud. Estimation of density distribution function of the apparent activation energy, *Int. J. Miner. Process.* 123, 46–59.
- [2] Snars, K., Gilkes, R.J., (2009). *Appl. Clay Sci.* 46, 13.
- [3] Thakur, R.S., Sant, B.R., (1983). *J. Sci. Ind. Res.* 42, 87.
- [4] Coutney, R., (2007). in: (Ed.), *Residue Solutions Pty Ltd.*
- [5] Meher, S. N., Rout, A. K., Padhi B. K., (2010). Extraction of Al and Na from Red Mud by Magnesium Oxide Sodium Carbonate Sinter Process. *Journal of Environmental Science and Technology*, 4, 897-902.
- [6] Zhong, L., Zhang, Y., Zhang, Yi., (2009). Extraction of Alumina and Sodium Oxide from Red Mud by a Mild Hydro-Chemical Process. *Journal of Hazardous Materials*, 172, 1629–1634.
- [7] Ghorbani, A., Fakharian, A., (2013). Recovery of Al<sub>2</sub>O<sub>3</sub>, Fe<sub>2</sub>O<sub>3</sub> and TiO<sub>2</sub> from Bauxite Processing Waste (Red Mud) by Using Combination of Different Acids. *Journal of Basic and Applied Scientific Research*, 3, 187-191.
- [8] Zhang, R., Zheng, S., Ma, S., Zhang, Yi., (2011). Recovery of Alumina and Alkali in Bayer Red Mud by The Formation of Andradite-Grossular Hydrogarnet in Hydrothermal Process. *Journal of Hazardous Materials*, 189, 827-835.
- [9] Xiao-bin, LI., Wei, X., Wei, L., Gui-hua, L., (2009). Recovery of Alumina and Ferric Oxide from Bayer Red Mud Rich in Iron by Reduction Sintering. *Transactions of Nonferrous Metals Society of China*, 19, 1342-1347.
- [10] Kresge, C.T., Leonowicz, M.E., Roth, W.J., Vartuli, J.C., Beck, J.C., (1992). Ordered

- mesoporous molecular sieves synthesized by a liquid–crystal template mechanism. *Nature*. 359, 710.
- [11] Kuemmel, M., Grosso, D., Boissiere, U., Smarsly, B., Brezesinski, T., Albouy, P.A. (2005). Thermally Stable Nanocrystalline  $\gamma$ -alumina Layers with Highly Ordered 3D Mesoporosity. *Angew. Chemical. International. Edition*. 44, 4589–4592.
- [12] Huang, F., Zheng, Y., Cai, G.H., Zheng, Y., Xiao, Y.H., Wei, K.M., (2010). A New Synthetic Procedure for Ordered Mesoporous  $\gamma$ -Alumina with a Large Surface Area. *Scr. Materials*. 63, 339–342.
- [13] Pan, F., Lu, X., Wang, T., Wang, Y., Zhang, Z., (2013). Synthesis of Large-Mesoporous  $\gamma$ -Al<sub>2</sub>O<sub>3</sub> from Coal-Series Kaolin at Room Temperature. *Materials Letters*. 91, 136-138.
- [14] Kim, J.H., Jung, K.Y., Park, K.Y., Cho, S.B., (2010). Characterization of mesoporous alumina particles prepared by spray pyrolysis of Al(NO<sub>3</sub>)<sub>2</sub>.9H<sub>2</sub>O precursor: Effect of CTAB and urea. *Journal of Microporous and Mesoporous Materials*. 128, 85-90.
- [15] Bagshaw, S.A., Pinnavaia, T.J., (1996). Mesoporous alumina molecular sieves. *Angew Chem Int Ed* 35, 1102 – 1105.

